American Journal of Mechanical Engineering, 2014, Vol. 2, No. 4, 120-124
Available online at http://pubs.sciepub.com/ajme/2/4/4

DOI:10.12691/ajme-2-4-4

Study on the Structure Deformation in the Process of Gas Metal Arc Welding (GMAW)

Pham Son Minh[1,*], Tran Viet Phu[2]

[1]University of Technical Education Ho Chi Minh City, HCM City, Vietnam
[2]Ho Chi Minh Vocational College of Technology, HCM City, Vietnam
*Corresponding author: minhps@hcmute.edu.vn

Received September 01, 2014; Revised September 11, 2014; Accepted September 18, 2014

Abstract This paper investigates the welding deformation via simulation and experiments. The structure of a combined joint geometry was modeled and simulated using Simufact welding software based on the thermo elastic–plastic approach. To verify the simulation results, a series of experiments was conducted with three different welding sequences using automated welding process, low carbon steel AISI 1005 as the parent metal, and digital gas metal arc welding (GMAW) power source with premixed shielding gas and the one-sided clamping technique. Based on the results, it was established that the thermo elastic–plastic 3D FEM analysis shows good agreement with experimental results, and the welding sequence "from inside to outside" induced less distortion compared with "from outside to inside". By claiming one plate, the deformation almost locates at the free plate.

Keywords: *welding simulation, structure deformation, heat transfer, plate connection, plate distortion*

Cite This Article: Pham Son Minh, and Tran Viet Phu, "Study on the Structure Deformation in the Process of Gas Metal Arc Welding (GMAW)." *American Journal of Mechanical Engineering*, vol. 2, no. 4 (2014): 120-124. doi: 10.12691/ajme-2-4-4.

1. Introduction

Metal plates are widely not only used to join actual welding structures in industry but also are normally accompanied by the addition of filler material as new weld passes e.g., single-pass welding process is often used considering a thin metal plate connection. In the welding field, predicting the structure deformation is one of the most important issues. This problem is often solved by the experiment of the weld designer.

In recent years, by numerical method, the structure deformation can be predicted. However, this makes it difficult to model the welding structure by the finite element method (FEM). Due to the intense concentration of heat in the heat source of welding, the regions near the weld line undergo many boundary condition as clamping force, heat transfer, heating source…, so, predicting three-dimensional weld deformation is a major topic for welding a variety of engineering alloys.

Full three-dimensional simulation of the arc welding process for predicting residual stresses is now feasible and practical, given recent developments in computing capabilities. Many researchers have studied the thermal distributions and residual stresses in welding. Teng et al. [1] studied about the residual stresses during multi-pass arc welding in steel pipes using finite element techniques and discussed the effects of pipe diameter and wall thickness on weld residual stresses. Adaptive mesh refinements were used to transport the results between the different meshes [2]. The thermo mechanical model used as well as the simulation methodology was detailed. Computed distortions and residual stresses were compared with experimental measurements. Butt-welding was simulated [3] for stainless steel pipes in a non-linear thermo mechanical FE analysis. In particular, the axial and hoop stresses and their sensitivity to variation in weld parameters were studied. In addition, a combined analytical and experimental method for analyzing the residual stresses in a pipe formed with a girth-butt weld was performed by many researched [4,5,6,7,8].

On the basis of simulating the single pass welding [9,10,11], the present investigation utilizes element "birth" and "death" finite element technique to control the process of filling metal step by step during welding process. At the same time, the dynamic thermal distributions and strain evolutions are analyzed in 10 mm plate-butt SUS310 stainless steel in multi-pass welding with FEM. The comparison between the calculated driving force and material resistance predict the weld metal deformation.

The objective of the present study is to develop an efficient method to reduce the design time and improve the accuracy for welding structure manufacturing. Therefore, a model considering both material properties and welding zone situation is analyzed. The local inherent stress of the welding bead is represented by an equivalent moment and other parameters, and then a new welding simulation software is proposed to predict the welding deformation.

2. Simulation and Experiment

Figure 1 shows the simulation procedure for GMAW. Base on this progression, the welding process will be designed according to the American Welding Society standards. Then, from the research model, the welding geometry can be created. All the welding models are meshed, and the boundary condition is also set up. All data will be used for the simulation running. Then, the software shows the result of temperature distribution, deformation, and the residual stress of all welding structures.

The evolution thermal analysis is quite a complex phenomenon associated with GMAW process. The weld pool shape can be largely influenced by the weld metal transfer mode and corresponding fluid flow dynamics [12]. In the representation of GMAW, the most widely acceptable double heat source model, presented by Goldak et al. [13], used for the FE modeling is shown in Figure 2. In this research, the parameters of Goldak's model are shown in Table 1. The chemical components of low carbon steel and its mechanical properties at room temperature are shown in Table 2 and 3, respectively.

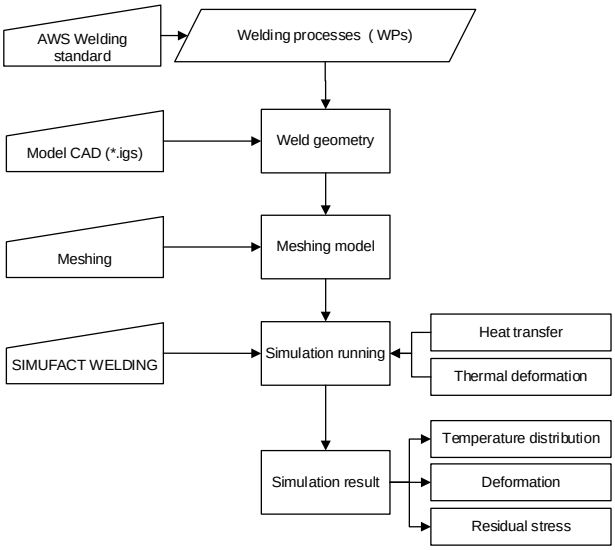

Figure 1. Simulation procedure

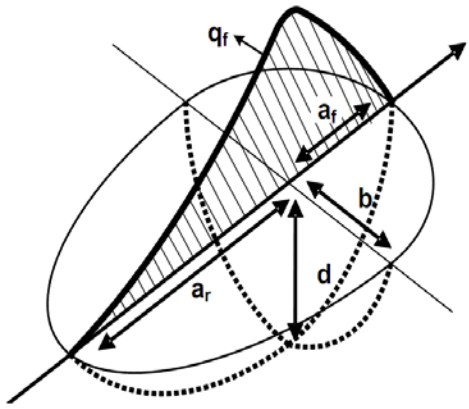

Figure 2. Goldak's model [12,13]

Table 1. Parameters of Goldak's double model

Parameters of Goldak's double ellipsoid	
a_f	4 mm
a_r	7 mm
b	3.5 mm
d	3 mm

Table 2. Chemical low carbon steel [12]

Standard	AISI 1005
% C	0.14–0.22
% Si	0.12–0.30
% Mn	0.40–0.65

Table 3. Material properties of welding plates [12]

Material properties	
Young's Modulus at 20°C	210 GPa
Minimum yield strength	355 MPa
Poisson's ratio	0.33
Solidus temperature	1404 °C
Liquidus temperature	1505 °C

Figure 3 shows the mesh of the welded plate used in the established 3D solid model. Fine mesh is used around weld path, but coarse mesh is used away from the weld. The initial condition involves preheating temperature, and all nodes are loaded except for fillers. Figure 4 shows the welding model with the original coordinate. The Y-axis is the plate width direction, the X-axis is the welding direction, and the Z-axis is the plate thickness direction. The units in weld zone are activated one by one during the welding process. The welding processes are shown as in Figure 5.

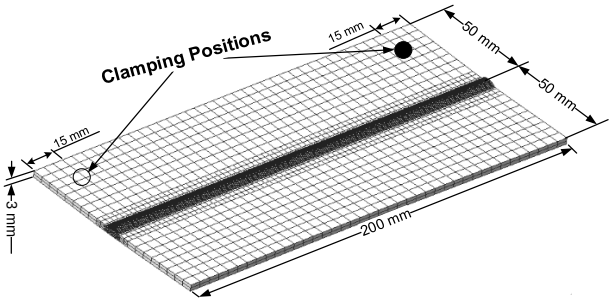

Figure 3. Mesh model for simulation

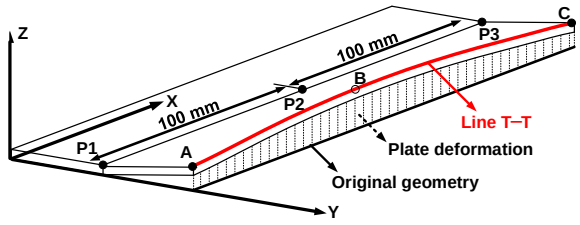

Figure 4. Location for observing the welding deformation

In this study, linear elastic shrinkage method using relatively new FEM software, SIMUFACT WELDING, developed by *Simufact Engineering GmbH*, is employed to simulate the welding process and to predict the welding distortion in a butt joint of thickness 3 mm. For verification, a series of experiments were also performed using a fully automated welding system with GMAW power source. The shielding gas for the welding process was carbon dioxide (CO2). To measure the initial and final dimensions of the specimen, a coordinate measuring machine was used. The welding parameters that have been used during the experiments are shown in Table 4. For observing the influence of welding process on the deformation of structure, three processes were designed for simulation and experiment. The description of welding

process is shown in Figure 5. First, two plates will be welded from point P1 to P3. Second, two plates will be welded from the outside to the center (point P2) of the weld path. Finally, two plates will be welded from the center (point P2) to the outside of the weld path.

Table 4. Welding parameters used for simulation and experimental method

Welding parameter	Value
Current	90 A
Voltage	21.6 V
Welding speed	5.7 mm/s

3. Results and Discussions

Plate's deformation at the end of the welding cycle is shown in Figure 6a and Figure 6b. With different processes, as shown in Figure 4, this result shows that the deformation of two plates is almost the same with different processes. The fixed plate has the smaller deformation than the free plate. The maximum deformation is located at line T–T (Figure 5). This result is because the clamping fore position and deformation of plate are strongly limited. Therefore, in the welding cycle, the thermal deformation decreased clearly. On the contrary, the free plate was deformed by the thermal stress. Figure 6a and Figure 6b also show that the free plate was bent to the welding side as shown in the 3D view, because of stress distribution. Because the weld only appears at the top surface, the stress distribution at the top surface is greater than those on the bottom surface because of the thermal imbalance of the two sides [14,15].

Process	Welding direction
1	P1 → P3
2	P1 → P2 ← P3
3	P1 ← P2 → P3

Figure 5. Welding processes

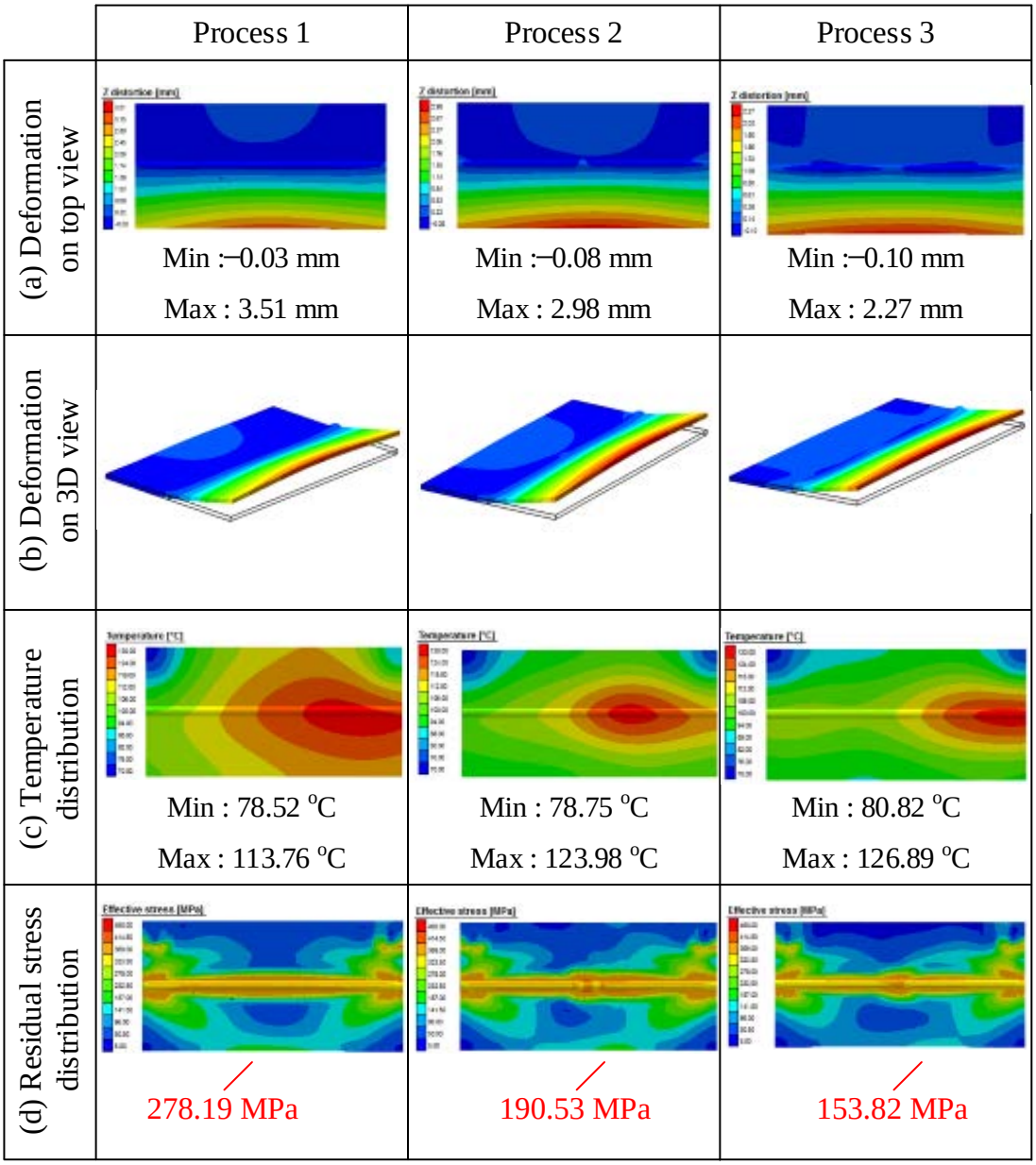

Figure 6. Simulation results at the end of the welding cycle

By comparing the deformation value between three processes, the results show that the maximum deformation was observed with process 1, which has the distortion ranging from −0.3 mm to 3.15 mm. This range decreased when process 2 and 3 was used. The reduction could be explained by thermal stress. In process 1, the thermal energy appeared at the welding line from point 1 to point 3. That is, with the same welding time, the plates in process 1 received continuously thermal energy, and the result was the heat concentrate appeared more clearly at the welding position, as shown in Figure 6c. Hence, the thermal stress is also greater than that of the other process, especially with the position of line T–T, as shown in Figure 6d. With process 2 and 3, although the welding time is the same with process 1, however, in these processes, the welding cycle includes two steps. Therefore, the heat concentration reduced clearly, and the residual stress decreased.

The plate deformation on line T–T is also studied. The results were collected and compared in Figure 7. Based on this result, it is clear that process 2 and 3 have greatly improved plate deformation. In addition, the deformation distribution on line T–T shows that the maximum distortion points are affected by the welding process.

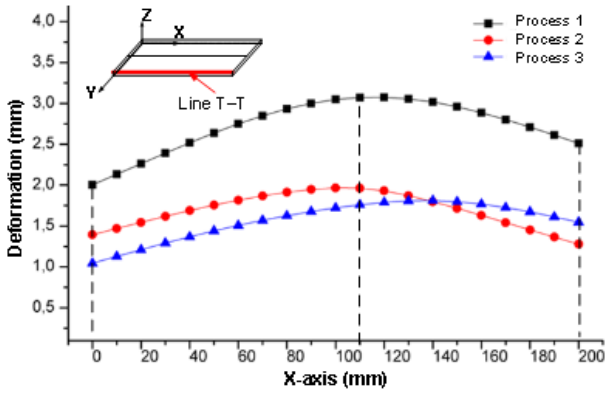

Figure 7. Simulation result of plate deformation on line T–T

In process 1, when the plates were welded continuously from point 1 to point 3, the larger deformation is located at the side of point 3. This result could be explained by thermal deformation. At the beginning of the welding cycle, both plates were cool. Therefore, the thermal deformation did not occur. However, when the welding process started, plates were heated, and the thermal deformation occurred. The longer the time for welding, the more the deformation. The temperature distribution can clearly be observed in Figure 6c. By simulation, the maximum distortion occurred at point 114.2 mm on X-axis.

In process 2 and 3, with two welding steps, the total deformation was reduced clearly because the thermal energy has more time to transfer to the other location in the plates. By comparing the deformation distribution, the maximum distortion in process 2 and 3 are located at the center (X = 102.6 mm) and to the right (X = 158.7 mm), respectively. The location of maximum deformation can be explained by the temperature distribution as well as residual stress. With process 2, the highest temperature is located between point 2 and 3 (Figure 6c), whereas with process 3, the highest temperature is located close to point 3 (Figure 6c). This difference in maximum temperature leads to the change in residual stress, as shown in Figure 6d. Therefore, the maximum deformation points of processes 2 and 3 appear at different positions.

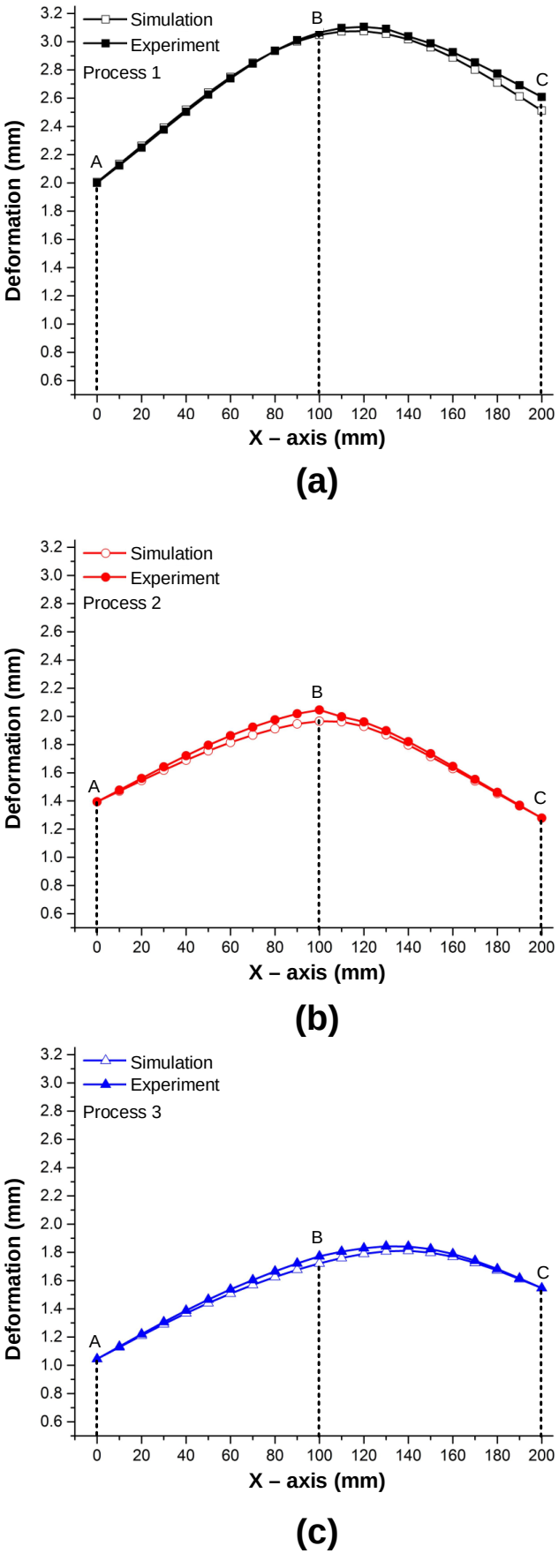

Figure 8. Plate deformation on line T–T with different processes

To verify the simulation accuracy, three GMAW processes were observed experimentally. Each process was performed 10 times. Then, the average deformation on line T–T was measured and compared with the simulation result. The experiment results are shown in Figure 8. Based on this result, the simulation and experiment have a good agreement. The difference between simulation and experiment occurs at different positions on line T–T. In process 1, 2, and 3, the difference is located near point C, B, and between point B and C. This result is because of the effect of the heat transfer coefficient and heat conductivity of the plate's material. In the simulation, these elements were given ideal values. However, in the experiment, these parameters cannot be exactly the same as those used in the simulation. In the experiment, because heat transfer is not as fast as the ideal material, at the end of welding cycle, the temperature of the real plate is higher than that of the simulation case. This is the main reason for the different deformations between the simulation and experiment.

4. Conclusions

In this study, a GMAW was performed on two metal plates. Three types of GMAW were established. The plate deformation was observed and compared with different processes. Based on these results, the following conclusions were obtained:

- By assuming the location of one plate, the deformation almost locates the free plate.
- With three processes, the deformation profiles are the same. However, the deformation values change considerably. The biggest deformation appears with the process 1 and reduces strongly with processes 2 and 3.
- By simulation, the distribution of temperature and stress were observed. This result explains the change of deformation under different processes.
- The deformation could be predicted by simulation accuracy.

Acknowledgements

The authors gratefully acknowledge the financial support for this research provided by the University of Technical Education Ho Chi Minh City, Vietnam.

References

[1] Teng, T. L., and Chang, P.H.,"A study of residual stresses in multi-pass girth-butt welded pipes", *International Journal of Pressure Vessels and Piping*, 74 (1). 59-70. November 1997.

[2] Duranton, P., Devaus, J., and Robin, V.,"3D modelling of multipass welding of a 316L stainless steel pipe", *Journal of Materials Processing Technology*, 153-154, 457-463. November 2004.

[3] Brickstad, B., and Josefson, B.L., "A parametric study of residual stresses in multi-pass butt-welded stainless steel pipes", *International Journal of Pressure Vessels and Piping*, 75 (1), 11-25. January 1998.

[4] Bouchard, P.J., and George, D., "Measurement of the residual stresses in a stainless steel pipe girth weld containing long and short repairs", *International Journal of Pressure Vessels and Piping*, 105 (4), 81-91. April 2005.

[5] Cho, J.R., Lee, B.Y., and Moon, Y.H., "Investigation of residual stress and post weld heat treatment of multi-pass welds by finite element method and experiments", *Journal of Materials Processing Technology*, 155-156, 1690-1695. November 2004.

[6] Elcoate, C.D., Dennis, R.J., and Bouchard, P.J., "Three dimensional multi-pass repair weld simulation", *International Journal of Pressure Vessels and Piping*, 82 (4), 244-257. April 2005.

[7] Shim, Y., Feng, Z., Lee, S., Kim, D., Jaeger, J., Papritan, J. C., and Tsai, C. L., "Determination of residual stresses in thick-section weldments", *Welding Journal*, 71, 305-312., September 1992.

[8] Murugan, S., Sanjai, K., Rai, B., and Kumar, P.V., "Temperature distribution and residual stresses due to multipass welding in type 304 stainless steel and low carbon steel weld pads", *International Journal of Pressure Vessels and Piping*, 78 (4), 307-317. April 2001.

[9] Bergmann, H., and Hilbinger, R., (1998) Numerical simulation of centre line hot cracks in laser beam welding of aluminum close to the sheet edge" in *International seminar; 4th, Numerical analysis of weld ability*, Institute of material, 658-668.

[10] Feng, Z.L., Zagharia, T., and David, S.A., "Thermal stress development in a nickel based super alloy during weld ability test", *Welding Journal*, 76, 470-483. November 1997.

[11] Feng, Z.L., and Tsai, C.L., "A computational analysis of thermal and mechanical conditions for weld metal solidification cracking", *Welding in the World*, 33 (5), 340-347. 1994.

[12] Goldak, J.A., and Akhlaghi, M., *Computational welding Mechanics*, SpringerPublishers, New York, USA, 2005.

[13] Goldak, J., Chakravarti, A., and Bibby, M., "A new finite element model for welding heat source", *InternationalJournal Metallurgical and Materials Transactions B*, 15 (2), 299-305. June 1984.

[14] Dong, Z.B., and Wei, Y.H., "Three dimensional modeling weld solidification cracks in multipass welding", *Theoretical and Applied Fracture Mechanics*, 46 (2), 56-165. October 2006.

[15] Zhang, H.J., Zhang, G.J., Cai, C.B., Gao, H.M., and Wu, L., "Numerical simulation of three-dimension stress field in double-sided double arc multipass welding process", *Materials Science and Engineering A*, 499 (1-2), 309-314. January 2009.